

Article

Characterization of the Mean First-Passage Time Function Subject to Advection in Annular-like Domains

Hélia Serrano ^{1,*}  and Ramón F. Álvarez-Estrada ^{2,†} 

¹ Departamento de Matemáticas, Facultad de Ciencias y Tecnologías Químicas, Universidad de Castilla-La Mancha, 13071 Ciudad Real, Spain

² Departamento de Física Teórica, Facultad de Físicas, Universidad Complutense de Madrid, 28040 Madrid, Spain; rfa@ucm.es

* Correspondence: heliac.pereira@uclm.es

† These authors contributed equally to this work.

Abstract: Cell migration in a biological medium towards a blood vessel is modeled, as a random process, successively inside an annulus (two-dimensional domain) and an annular cylinder (three-dimensional domain). The conditional probability function u for the cell moving inside such domains (tissue) fulfills by assumption a diffusion–advection equation that is subject to a Dirichlet boundary condition on the outer boundary and a Robin boundary condition on the inner boundary. The mean first-passage time (MFPT) function determined by u estimates the average time for the travelling cell to reach various interesting targets. The MFPT function fulfills a Poisson equation inside a domain with suitable boundary conditions, which give rise to various mathematical problems. The main novelty of this study is the characterization of such an MFPT function inside an annulus and an annular cylinder, which is subject to a Robin boundary condition on the inner boundary and a Dirichlet boundary condition on the outer one, and these are integral functions whose densities are the solution of an inhomogeneous system of linear integral equations.

Keywords: mean first-passage time; diffusion–advection equation; Dirichlet and Robin boundary conditions; annulus; annular cylinder

MSC: 35K20; 45F05; 92C17



Citation: Serrano, H.; Álvarez-Estrada, R.F. Characterization of the Mean First-Passage Time Function Subject to Advection in Annular-like Domains. *Mathematics* **2023**, *11*, 4998. <https://doi.org/10.3390/math11244998>

Academic Editor: Giancarlo Consolo

Received: 16 November 2023

Revised: 11 December 2023

Accepted: 14 December 2023

Published: 18 December 2023



Copyright: © 2023 by the authors. Licensee MDPI, Basel, Switzerland. This article is an open access article distributed under the terms and conditions of the Creative Commons Attribution (CC BY) license (<https://creativecommons.org/licenses/by/4.0/>).

1. Introduction

Cell migration is a key process in a variety of biological phenomena, from embryonic development to immune responses and even cancer metastasis, as well as an inherently complex process influenced by multiple factors, including cell type, environmental conditions, and interactions with other cells or extracellular matrix components. See [1–6]. These factors can create different modes of migration that can be understood using statistical physics frameworks, especially the idea of random walks. Random-walk models consider cells as random walkers whose displacement is governed by both diffusion and advection, and they have been effectively used to describe the statistical behavior of cell migration. Diffusion accounts for the random, undirected component of cell movement, thus originating from the intrinsic stochasticity of the intracellular machinery. Advection, on the other hand, describes directed cell migration, such as chemotaxis where cells move along a chemical concentration gradient. See [7]. As a result, understanding the dynamics of cell migration is a fundamental problem in biological physics.

The mean first-passage time (MFPT) in cell migration refers to the average time it takes for a cell to reach a specific target location or cross a defined boundary for the first time. See [8–10]. The MFPT, fulfilling a Poisson equation subject to mixed Dirichlet–Neumann boundary conditions in different confined domains, has been widely studied in the last decades from analytical and numerical points of view. See [11,12] and their references. For

instance, the study of the upper and lower bounds of the MFPT of a cell escape through a boundary region, satisfying a diffusion equation under mixed Dirichlet–Neumann boundary conditions, has been undertaken in [13]. The study of the asymptotic behavior of the MFPT in annulus geometries with inner and outer regions has been carried out in [14]. The characterization of the MFPT function in three-dimensional simply and doubly connected domains subject to Dirichlet and Neumann boundary conditions has been achieved previously in [15] by means of a system of inhomogeneous linear integral equations.

In this work, we consider a tissue filling a nonsimply connected finite domain Ω and bounded by a smooth closed boundary Γ . Inside Ω , a cell migrates towards a certain part of Γ so as to intravasate it into a blood vessel located outside Ω , and it is enclosed by Ω . The cell is subject to both diffusive and drift motions, the latter of which are characterized by a suitable vector v whose magnitude will be assumed to be small. Let x and y be two arbitrary points in Ω . The conditional probability density (or transition probability) of a cell to be at x at time $t \geq 0$, being originated at y at time $t = 0$, is supposed to be the solution $u(t, x, y)$ of the diffusion–advection equation

$$\left(\frac{\partial}{\partial t} - D(\Delta_x + v \cdot \nabla_x)\right)u(t, x, y) = 0, \tag{1}$$

where $D > 0$ is the diffusion coefficient, which is subject to the following conditions:

- (A1) $u(0, x, y) = \delta(x - y)$ for any $x, y \in \Omega$;
- (A2) $\lim_{t \rightarrow +\infty} \int_{\Omega} u(t, x, y) dx = 0$ for any $y \in \Omega$.

Here, δ stands for the Dirac delta function. The diffusion–advection equation describes the spatiotemporal behavior of cells undergoing both diffusion (random motion) and advection (directed motion) due to external factors, such as chemotaxis (movement in response to chemical gradients) or mechanical forces within the domain Ω .

The MFPT function T , at $y \in \Omega$, is defined as

$$T(y) = \int_{\Omega} \int_0^{+\infty} u(t, x, y) dt dx, \tag{2}$$

where u is the solution of (1), which is subject to conditions (A1) and (A2). The MFPT function quantifies the average time it takes for a migrating cell to reach the domain boundary, which provides a probabilistic measure of the expected time for a cell to achieve a particular outcome, which is essential for understanding cell behavior and navigation.

Moreover, consider that z is a point on the boundary Γ , and let $n(z)$ be the inner normal-unit vector at z on Γ , and let the product $n(z) \cdot \nabla f(z) \equiv \frac{\partial f(z)}{\partial n(z)}$ be the inner first derivative of the function f at z on Γ . Assume that there are two disjoint regions Γ_D and Γ_R on the boundary Γ so that $\Gamma = \Gamma_D \cup \Gamma_R$, and the following boundary conditions are satisfied:

- (B1) (Dirichlet) $\lim_{y \rightarrow z} f(y) = 0$, for any z in a region $\Gamma_D \subset \Gamma$,
- (B2) (Robin) $a \lim_{y \rightarrow z} \frac{\partial f(y)}{\partial n(y)} + b \lim_{y \rightarrow z} f(y) + c = 0$ for any z in a region $\Gamma_R \subset \Gamma$, with $a \neq 0$, b , and c given as real constants.

The Dirichlet and Robin boundary conditions describe how cells interact with the boundaries of the domain. The Dirichlet boundary condition (B1) prevents cells from leaving or entering through such a boundary so that they are constrained to remain within the tissue Ω . The Robin boundary condition (B2) is expressed as a combination of both the Dirichlet and Neumann boundary conditions. The Dirichlet component of the Robin boundary condition prevents cells from leaving or entering the domain, while the Neumann component accounts for the flux of cells at the boundary and represents the rate at which cells are allowed to move across such a boundary.

Notice that, in the MFPT function, the T defined in (2) solves the so-called adjoint equation

$$D(\Delta + v \cdot \nabla)T(y) = -1 \tag{3}$$

in Ω , which is subject to the boundary conditions (B1) and (B2) and the finiteness condition $0 \leq T(y) < +\infty$ in Ω . This is a direct generalization of the result, without drift ($|v| = 0$), as stated in [15] (Proposition 2.3). See also [16,17].

Our aim is to first characterize the MFPT function when the domain Ω is an annulus and then when it is an annular cylinder, thereby assuming the Dirichlet boundary condition (B1) on the outer boundary and the Robin boundary condition (B2) on the inner one. Therefore, in the next section, the explicit characterization of the MFPT function is achieved, assuming drift motion, when the domain is an annulus limited by two closed and nonintersecting curves. This domain intends to model the orthogonal projection into a plane of the tissue and the blood vessel. Then, in Section 3, the three-dimensional domain considered is an annular cylinder filled by tissue, which surrounds the blood vessel, thereby assuming no drift motion, for simplicity and satisfying the Dirichlet boundary condition (B1) on the outer boundary surface and the Robin boundary condition (B2) on the inner one. The main novelty in this study is to consider a diffusion–advection equation that is subject to a Robin boundary condition on the inner boundary of an annulus and an annular cylinder. In the last sections, the conclusions are stated and discussed. Supplementary justifications and discussions are presented in Appendices A and B for the two-dimensional case and in Appendix C for the three-dimensional one.

2. The MFPT Function in an Annulus

In this section, let us consider the following two dimensional domains:

- The domain Ω_1 is an annulus enclosed by two concentric circles σ_1 and σ_2 , with radii r_1 and r_2 , respectively ($r_1 \leq r_2$), so that the boundary is formed by the union of such circles;
- The domain Ω_2 is enclosed by two arbitrary smooth (differentiable) curves σ_3 and σ_4 , which are obtained as small deformations of the previous concentric circles σ_1 and σ_2 , respectively.

The first situation corresponds to a very idealized planar geometry for the tissue surrounding the blood vessel, while the second one tries to simulate a somewhat less-idealized planar geometry for the cross-section. Assume a radial drift on the cell directed towards the origin of coordinates, that is, $v = -\frac{|v|}{\rho} y$.

Proposition 1. Consider the domain Ω_1 with the Dirichlet boundary condition (B1) on the outer circle σ_2 and the Robin boundary condition (B2) on the inner circle σ_1 . The MFPT function T_1 is given by

$$T_1(\rho) = \left(\alpha_2 + \frac{1}{D|v|^2} \right) \int_{\rho}^{r_2} \frac{e^{|\nu|\xi}}{\xi} d\xi - \frac{1}{D|v|^2} \ln\left(\frac{r_2}{\rho}\right) - \frac{r_2 - \rho}{D|v|}, \tag{4}$$

for every $\rho \in [r_1, r_2]$ for a suitable integration constant α_2 so that $a \lim_{\rho \rightarrow r_1} \frac{dT_1(\rho)}{d\rho} + b \lim_{\rho \rightarrow r_1} T_1(\rho) + c = 0$.

Proof. Upon taking the common center of σ_1 and σ_2 as the origin, the standard plane polar coordinates $\rho \geq 0$ and $\varphi \in [0, 2\pi)$ will be chosen so that $y = \rho(\cos \varphi, \sin \varphi)$. Then, the adjoint Equation (3) may be written as

$$\left(\frac{1}{\rho} \frac{\partial}{\partial \rho} \left(\rho \frac{\partial}{\partial \rho} \right) + \frac{1}{\rho^2} \frac{\partial^2}{\partial \varphi^2} - |v| \frac{\partial}{\partial \rho} \right) T(\rho, \varphi) = -\frac{1}{D}. \tag{5}$$

If the MFPT function has circular symmetry, that is, it is φ -independent, then it may be defined as $T_1(\rho)$, thus being the solution of

$$\left(\frac{1}{\rho} \frac{d}{d\rho} \left(\rho \frac{d}{d\rho}\right) - |\nu| \frac{d}{d\rho}\right) T_1(\rho) = -\frac{1}{D}, \tag{6}$$

which is a nonself-adjoint second-order linear differential equation. Without needing to transform it to a self-adjoint form, it can be solved directly so that

$$T_1(\rho) = \alpha_1 + \alpha_2 \int_{\rho}^{r_2} \frac{e^{|\nu|\xi}}{\xi} d\xi + \frac{1}{D} \int_{\rho}^{r_2} \frac{e^{|\nu|\xi}}{\xi} \left[\left(\frac{1 - e^{-|\nu|\xi}}{|\nu|}\right) \xi + \frac{1}{|\nu|} \left(\frac{1 - e^{-|\nu|\xi}}{|\nu|} - \xi\right) \right] d\xi,$$

where α_1 and α_2 are alternative pairs of arbitrary integration constants. Now, taking into account the boundary conditions, it follows that if the Dirichlet condition (B1) is assumed when $\rho = r_2$ on the circle σ_2 , then $T_1(r_2) = 0$. Particularly, $\alpha_1 = 0$. If the Robin boundary condition (B2) is imposed when $\rho = r_1$ on the circle σ_1 , it follows that $a \lim_{\rho \rightarrow r_1} \frac{dT_1(\rho)}{d\rho} + b \lim_{\rho \rightarrow r_1} T_1(\rho) + c = 0$, since $\frac{\partial}{\partial n(z)} = \frac{d}{d\rho}$, which gives an expression for α_2 . Simplifying it follows (4). \square

As a particular case of the previous result, suppose two homogeneous Dirichlet boundary conditions that assume conditions (B1) and (B2), with $a = c = 0$ and $b = 1$, and make a change of the variable $\eta = |\nu|\rho$ with $\eta_1 = |\nu|r_1$ and $\eta_2 = |\nu|r_2$. The maximum of $D|\nu|^2 T_1(\eta)$ is obtained at the root of the implicit equation:

$$1 + \eta - \frac{(\eta_2 - \eta_1 + \ln(\frac{\eta_2}{\eta_1}))e^\eta}{\int_{\infty}^{\eta_2} \frac{e^t}{t} dt - \int_{\infty}^{\eta_1} \frac{e^t}{t} dt} = 0.$$

When $\eta_1 = |\nu|r_1 = 5$ and $\eta_2 = |\nu|r_2 = 50$, Figure 1 displays the function $D|\nu|^2 T_1(\eta)$.

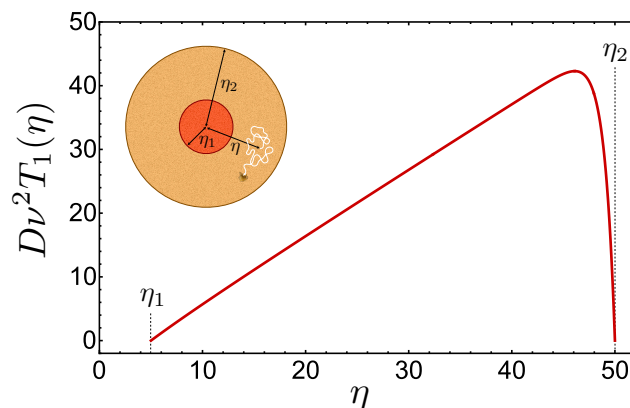


Figure 1. The maximum MFPT is attained near the circle σ_2 , thereby assuming Dirichlet boundary condition (B1) on both circles σ_1 and σ_2 .

Now, as a less-idealized planar geometry for the projections of a tissue and the blood vessel onto an orthogonal plane to the latter, suppose that the arbitrary smooth curves σ_3 and σ_4 are approximately close to (or do not differ much from) two concentric circles σ_1 and σ_2 , respectively. In other words, σ_3 and σ_4 are small or moderate deformations of σ_1 and σ_2 , respectively. Consequently, the common center of the circles σ_1 and σ_2 , even if not an exact center of symmetry for σ_3 and σ_4 , does not differ much from a point playing such a role. Let Ω_2 be the domain enclosed by σ_3 and σ_4 , and let that inside the annulus be Ω_1 . The following representation of the MFPT function T_2 in (7) is given as the sum of a particular solution T_1 throughout all Ω_1 , which is characterized in (4), plus as a general solution inside

Ω_2 of the homogeneous equation $D(\Delta + \nu \cdot \nabla)T(y) = 0$, which is expressed as the sum of two closed-line integrals along σ_3 and σ_4 containing the densities μ_2 and μ_1 , respectively.

Theorem 1. Consider the domain Ω_2 , with the Dirichlet boundary condition (B1) on the outer curve σ_4 and the Robin boundary condition (B2) on the inner curve σ_3 . The MFPT function T_2 is given by

$$T_2(y) = T_1(|y|) + \frac{2D}{a} \int_{\sigma_3} G(y, \xi) \mu_1(\xi) d\sigma(\xi) - 2D \int_{\sigma_4} \frac{\partial G(y, \xi)}{\partial n(\xi)} \mu_2(\xi) d\sigma(\xi), \tag{7}$$

for every $y \in \Omega_2$, where T_1 is defined in (4), G is the Green’s function, and the densities μ_1 and μ_2 are solutions of the system

$$\begin{aligned} \mu_1(\xi) = & \left(a \frac{\partial}{\partial n(\xi)} + b \right) \left(\frac{2D}{a} \int_{\sigma_3} G(\xi, s) \mu_1(s) d\sigma(s) - 2D \int_{\sigma_4} \frac{\partial G(\xi, s)}{\partial n(s)} \mu_2(s) d\sigma(s) \right) + \\ & + \left(a \frac{\partial}{\partial n(\xi)} + b \right) T_1(|\xi|) + c, \tag{8} \end{aligned}$$

$$\mu_2(\xi) = T_1(|\xi|) + \frac{2D}{a} \int_{\sigma_3} G(\xi, s) \mu_1(s) d\sigma(s) - 2D \int_{\sigma_4} \frac{\partial G(\xi, s)}{\partial n(s)} \mu_2(s) d\sigma(s). \tag{9}$$

Proof. Let $G(y, y')$ be the Green’s function, at (y, y') in the whole plane, so that

$$D(\Delta_y + \nu \cdot \nabla_y)G(y, y') = -\delta(y - y'), \tag{10}$$

where δ stands for the two-dimensional Dirac delta function, without any sort of Dirichlet or Robin boundary conditions either on σ_2 or σ_1 , nor on σ_4 or σ_3 . Notice that G includes angular dependences, which are certainly relevant for what follows. If $|\nu| = 0$, then it follows that

$$G(y, y')|_{|\nu|=0} = -\frac{1}{2\pi D} \ln|y - y'|, \tag{11}$$

which has a logarithmic singularity as $|y - y'|$ tends to 0.

The crucial features to obtain the density μ_2 are explained below. Consider two close points ξ and z lying on a small-line element δ_4 on the curve σ_4 and a point y lying inside Ω_2 and close to z so that the difference between $I(y)_{\delta_4}$ and $I(z)_{\delta_4}$ of the line integrals on δ_4 is

$$I(y)_{\delta_4} - I(z)_{\delta_4} = \int_{\delta_4} \frac{\partial G(y, \xi)}{\partial n(\xi)} d\sigma(\xi) - \int_{\delta_4} \frac{\partial G(z, \xi)}{\partial n(\xi)} d\sigma(\xi). \tag{12}$$

According to Appendix A, the Green’s functions G (including drift) and $G|_{|\nu|=0}$ (with vanishing drift) have the same short-distance behavior, since the operator $\nu \cdot \nabla$ is a weak perturbation of Δ . Then, it is permissible to replace G with $G|_{|\nu|=0}$ in (12). The resulting integrals in (12) are extended to the complete closed curve σ_4 . The added contributions to both integrals cancel out with each other. Thus, $I(y)_{\delta_4} - I(z)_{\delta_4} = I(y)_{\sigma_4} - I(z)_{\sigma_4}$, with

$$I(y)_{\sigma_4} - I(z)_{\sigma_4} = -\frac{1}{2\pi D} \left(\int_{\sigma_4} \frac{\partial \ln|y - \xi|}{\partial n(\xi)} d\sigma(\xi) - \int_{\sigma_4} \frac{\partial \ln|z - \xi|}{\partial n(\xi)} d\sigma(\xi) \right).$$

Except for $(2\pi D)^{-1}$, these closed-line integrals are the full angles determined by the whole σ_4 as seen from two situations: either a point y lying strictly inside Ω_2 , close to z , or inside z . By directly extending the argument in [18], those two dimensional angles are 2π and π , respectively. This statement will be illustrated through the following simple example. Let σ_4 be a circle of radius r_4 , and let y be its center. Therefore, as $\frac{\partial}{\partial n(\xi)}$ denotes the inner normal derivative and $|\xi| = r_4$, it follows that $2\pi D I(y)_{\sigma_4} = \int_{\sigma_4} \frac{1}{|\xi|} d\sigma(\xi) = 2\pi$.

The actual counterpart of $I(z)_{\sigma_4}$, if the closed-line σ_4 is the boundary of a half circle and z is taken at the center, yields π . Thus, all that leads to the characterization of the density μ_2 by (9). The extension of the above justification to the characterization of the density μ_1 to the actual closed curve σ_3 in two dimensions with the drift and Robin boundary condition can also be carried out directly. For brevity, it will be omitted here. \square

Models in two dimensions are plagued by a number of subtleties compared to models in three dimensions, as shown in the following very simplified model in Example 1, where the domain is only one circle. The structure of the integral equation approach in the proof of Theorem 1 is confirmed, and the important “averaging” recipe is introduced.

Example 1. Let Ω now be the interior of the full circle σ_2 of radius r_2 , inside of which a cell moves randomly without drift, with the Dirichlet boundary condition. The circle σ_1 and, therefore, the Robin boundary condition are eliminated in this example. Accepting circular symmetry, the MFPT function T_1 solving Equation (6), with the Dirichlet boundary condition, is defined as follows:

$$T_1(\rho) = \frac{r_2^2 - \rho^2}{4D}. \tag{13}$$

Consistency will be achieved if (13) is retrieved out of the following modified simplifications of (7) and (9). Namely, if the MFPT function T_2 is defined in (7), for any $y \in \Omega$ and taking the density μ_2 given in (9), then

$$T_2(y) = T_1(|y|) - 2D \int_{\sigma_2} \frac{\partial G(y, \xi)}{\partial n(\xi)} \mu_2(\xi) d\sigma(\xi) \tag{14}$$

with

$$\mu_2(\xi) = T_1(|\xi|) - 2D \int_{\sigma_2} \frac{\partial G(\xi, s)}{\partial n(s)} \mu_2(s) d\sigma(s), \tag{15}$$

where $T_1(|y|) = -\frac{|y|^2}{4D}$, without drift. The density μ_2 has supposed consistency, which depends only on $\rho = |\xi|$. By using (A1), (A5), and (15), noticing that the normal derivative is the inner one (towards the interior of the domain), and integrating over the angles (so that only $g_0(\rho, \rho')$ contributes), it follows that

$$\mu_2(\xi) = T_1(|\xi|) - 2Dr_2\mu_2(r_2) \frac{\partial \ln \rho_{max}(\rho, r_2)}{\partial \rho'} \tag{16}$$

where $\rho_{max}(\rho, \rho') = \max\{\rho, \rho'\}$. When $\rho' = r_2$, the derivative $\frac{\partial \ln \rho_{max}(\rho, r_2)}{\partial \rho'}$ is ambiguous so that some prescription will be required to handle it. By applying the “averaging” recipe in [15], we have

$$\frac{\partial \ln \rho_{max}(\rho, r_2)}{\partial \rho'} = \frac{1}{2} \left(\frac{\partial \ln \rho_{max}(\rho^+, \rho')}{\partial \rho'} + \frac{\partial \ln \rho_{max}(\rho^-, \rho')}{\partial \rho'} \right),$$

where the first and second terms are evaluated for $\rho^+ = \rho > \rho'$ and $\rho^- > \rho = \rho'$, respectively. The result is then $\frac{1}{2\rho'}$, which becomes $\frac{1}{2r_2}$. In this way, the density μ_2 in (16) is given by $\mu_2(\xi) = \frac{r_2^2}{4D}$. So, the second term on the right-hand side of (16) is of the same order as the left-hand side. The integral in (14) is directly computed for y inside Ω , which also uses $g_0(\rho, \rho')$ so that the above ambiguity does not arise. Therefore, $T_2(y) = T_1(|y|) + \frac{r_2^2}{4D}$, which consistently agrees with (13).

In Appendix B, an approximation method to characterize the densities μ_1 and μ_2 is presented whenever the curves σ_3 and σ_4 are close to the circles σ_1 and σ_2 , respectively.

3. The MFPT Function in an Annular Cylinder

In this section, the three-dimensional domain is an annular cylinder filled by tissue, where a cell migrates inside it towards the blood vessel surrounded by it when there is no drift, that is, $|\nu| = 0$ for simplicity. Namely, we consider the following cases:

- The domain Ω_3 is an annular cylinder limited by two parallel and concentric cylindrical surfaces S_1 and S_2 , with radii r_1 and r_2 , respectively, with $r_1 < r_2$, and by two lids. Precisely, they are the finite intersections of two parallel planes (at a distance h from each other) with the cylinders and orthogonal to the axes of the latter; see Figure 2 below;
- By letting the two lids, in the previous case, be very separated from each other (as if h tends to infinity) so that they can be disregarded, the surface boundary will be supposed to be a small or moderate deformation of the two cylindrical surfaces in scenario 3.

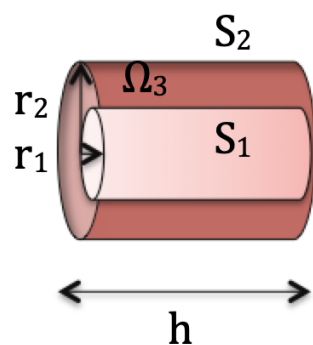


Figure 2. The annular cylinder Ω_3 bounded by the inner surface S_1 and the outer surface S_2 .

The domain Ω_3 corresponds to a very idealized cylindrical geometry for the tissue surrounding the blood vessel so that its analysis will rely on and constitute a nontrivial extension to three dimensions of the domain Ω_1 , which was defined in the previous section.

Proposition 2. Consider the domain Ω_3 , with the Dirichlet boundary condition (B1) on the outer surface S_2 and the Robin boundary condition (B2) on the inner surface S_1 . The MFPT function T_3 is characterized in Ω_3 , using cylindrical coordinates, by

$$T_3(\rho, z) = -\frac{2c_4}{h} \int_0^{+\infty} \sum_{k_z} \sin\left(k_z \frac{h}{2}\right) \frac{f_{k_\rho}(\rho) f_{k_z}(z) k_\rho}{k_\rho^2 + k_z^2} \frac{k_\rho}{k_z} [c_1(r_2 J_1(k_\rho r_2) - r_1 J_1(k_\rho r_1)) + c_2(r_2 Y_1(k_\rho r_2) - r_1 Y_1(k_\rho r_1))] dk_\rho,$$

where $f_{k_\rho}(\rho) = c_1 J_0(k_\rho \rho) + c_2 Y_0(k_\rho \rho)$, $f_{k_z}(z) = c_3 \sin(k_z z) + c_4 \cos(k_z z)$, with J_i and Y_i , for $i \in \{0, 1\}$ being the standard regular and irregular Bessel functions of the i th order, respectively, for constants c_1, c_2 , and c_4 , which are determined by the boundary conditions.

Proof. Let σ_1 and σ_2 be two concentric circles with radii r_1 and r_2 , respectively, so that $r_1 < r_2$, which are formed by the intersection of a plane with the two cylindrical surfaces S_1 and S_2 orthogonal to them, respectively. Upon taking the common center of σ_1 and σ_2 as the origin of the coordinates, the z axis through that point will be orthogonal to that plane. Consider the standard cylindrical coordinates $w = (\rho, \varphi, z)$, with $y = (\rho \cos \varphi, \rho \sin \varphi, z)$, so that the three-dimensional domain Ω_3 may be defined as $r_1 < \rho < r_2, 0 \leq \varphi < 2\pi$, and $-\frac{h}{2} < z < \frac{h}{2}$. Then, the Laplacian operator in (3) may be written as

$$\Delta = \frac{1}{\rho} \frac{\partial}{\partial \rho} \left(\rho \frac{\partial}{\partial \rho} \right) + \frac{1}{\rho^2} \frac{\partial^2}{\partial \varphi^2} + \frac{\partial^2}{\partial z^2}.$$

Thus, take into account a MFPT function $T_3(\rho, z)$ with circular symmetry (φ -independent) solution of

$$\left(\frac{1}{\rho} \frac{\partial}{\partial \rho} \left(\rho \frac{\partial}{\partial \rho}\right) + \frac{\partial^2}{\partial z^2}\right) T_3(\rho, z) = -\frac{1}{D} \tag{17}$$

in Ω_3 . In addition, consider the Dirichlet boundary condition (B1), when $\rho = r_2$, so that $T_3(r_2, z) = 0$, and consider the Robin boundary condition (B2), for $\rho = r_1$, so that $a \lim_{\rho \rightarrow r_1} \frac{\partial T_3(\rho, z)}{\partial \rho} + b \lim_{\rho \rightarrow r_1} T_3(\rho, z) + c = 0$ for some constants a, b , and c . On the lids, when $z = -\frac{h}{2}$ and $z = \frac{h}{2}$, assume a homogeneous Robin boundary condition so that $a \lim_{\rho \rightarrow r_1} \frac{\partial T_3(\rho, \pm \frac{h}{2})}{\partial \rho} + b \lim_{\rho \rightarrow r_1} T_3\left(\rho, \pm \frac{h}{2}\right) = 0$. For simplicity, the constants a and b are taken to be the same for the Robin boundary conditions at $\rho = r_1$ and at the two lids. The generalization for the different constants is direct and will be omitted.

The procedure to find out the MFPT function T_3 proceeds by applying well-documented procedures based upon suitable three-dimensional Green’s functions and representations thereof using separability, factorization, and eigenfunctions; see [19]. Thus, let $G_3(w, w')$ be the Green’s function, in cylindrical coordinates, solution of the equation

$$D \left(\frac{1}{\rho} \frac{\partial}{\partial \rho} \left(\rho \frac{\partial}{\partial \rho}\right) + \frac{\partial^2}{\partial z^2}\right) G_3(w, w') = -\frac{1}{\rho} \delta(\rho - \rho') \delta(z - z'),$$

so that

$$G_3(w, w') = \int \sum_{k_z} \frac{f_{k_\rho}(\rho) f_{k_z}(z) f_{k_\rho}(\rho') f_{k_z}(z')}{k_\rho^2 + k_z^2} dk_\rho,$$

with

$$\int \sum_{k_z} f_{k_\rho}(\rho) f_{k_z}(z) f_{k_\rho}(\rho') f_{k_z}(z') dk_\rho = \frac{1}{\rho} \delta(\rho - \rho') \delta(z - z') \tag{18}$$

$$D \left(\frac{1}{\rho} \frac{d}{d\rho} \left(\rho \frac{d}{d\rho}\right)\right) f_{k_\rho}(\rho) = -k_\rho^2 f_{k_\rho}(\rho) \tag{19}$$

$$D \frac{d^2 f_{k_z}(z)}{dz^2} = -k_z^2 f_{k_z}(z). \tag{20}$$

The solutions of Equations (19) and (20) may be written as $f_{k_\rho}(\rho) = c_1 J_0(k_\rho \rho) + c_2 Y_0(k_\rho \rho)$, where J_0 and Y_0 are the standard regular and irregular Bessel functions, respectively, of the zeroth order, and $f_{k_z}(z) = c_3 \sin(k_z z) + c_4 \cos(k_z z)$ for constants c_1, c_2, c_3 , and c_4 , which are determined by imposing the boundary conditions. The boundary conditions for $f_{k_\rho}(\rho)$ at r_1 (inhomogeneous Robin condition) and r_2 (Dirichlet condition) are similar to those in the two-dimensional case for $|\nu| \neq 0$, and they will not be repeated again. In the case of the Robin boundary condition, if $c \neq 0$, then k_ρ (real) varies continuously, and the constants c_1 and c_2 are uniquely defined by the inhomogeneous system. On the other hand, the homogeneous Robin boundary conditions for $f_{k_z}(z)$ at $z = \pm \frac{h}{2}$ make Equation (20) yield an eigenvalue equation for k_z , which has to take on a denumerably infinite set of values with the alternative choices: either $c_3 = 0$ and $c_4 \neq 0$ for the eigenvalue equation $\tan(k_z \frac{h}{2}) = -\frac{b}{a k_z}$ or $c_3 \neq 0$ and $c_4 = 0$ for the eigenvalue equation $\tan(k_z \frac{h}{2}) = \frac{a k_z}{b}$. The nonvanishing proportionality constant is determined through the completeness of Equation (18). Now, if the integration over ρ' and z' is performed, it follows, for $c_3 = 0$, that

$$\begin{aligned}
 T_3(\rho, z) &= - \int_{r_1}^{r_2} \int_{-\frac{z_0}{2}}^{\frac{z_0}{2}} \rho' G_3(w, w') dz' d\rho' = \\
 &= - \int_0^{+\infty} \sum_{k_z} c_4 \frac{f_{k_\rho}(\rho) f_{k_z}(z) \sin\left(k_z \frac{h}{2}\right)}{k_\rho^2 + k_z^2} \frac{1}{k_z \frac{h}{2}} (c_1 k_\rho (r_2 J_1(k_\rho r_2) - \\
 &\quad r_1 J_1(k_\rho r_1)) + c_2 k_\rho (r_2 Y_1(k_\rho r_2) - r_1 Y_1(k_\rho r_1))) dk_\rho,
 \end{aligned}$$

where J_1 and Y_1 are the standard regular and irregular Bessel functions of the first order, respectively. In this way, the MFPT function is characterized in terms of an integral and a series. If $\frac{h}{2}$ tends to $+\infty$, the description in the two-dimensional case for $|v| = 0$ is retrieved. \square

Now, let us consider the domain Ω_4 , where the geometry of the domain Ω_3 is considered and the two lids are suppressed so that the two cylindrical surfaces S_1 and S_2 extend along $-\infty < z < +\infty$. The boundary surface of the three-dimensional domain Ω_4 is formed by two surfaces, which are denoted by S_3 and S_4 and are very lengthy and moderate deformations of the above S_1 and S_2 , respectively. Upon recalling that Ω_3 encloses Ω_4 , the MFPT function T_4 defined below in (21) is the sum of a particular solution T_1 defined in (4) throughout all Ω_3 , plus it is a solution of $D\Delta T(y) = 0$ inside Ω_4 , which is expressed as the sum of two surface integrals along S_3 and S_4 containing μ_3 and μ_4 , respectively. Notice that the MFPT function T_4 and the densities μ_3 and μ_4 are, in particular, z -dependent. When $S_i = S_{i-2}$, for $i \in \{3, 4\}$, then $\mu_3 = 0$ and $\mu_4 = 0$, trivially.

Theorem 2. Consider the domain Ω_4 with the Dirichlet boundary condition (B1) on the outer surface S_4 and the Robin boundary condition (B2) on the inner surface S_3 . The MFPT function T_4 is characterized in Ω_4 by

$$T_4(y) = T_1(|y|) + \frac{2D}{a} \int_{S_3} G_3(y, x) \mu_3(x) dS(x) - 2D \int_{S_4} \frac{\partial G_3(y, x)}{\partial n(x)} \mu_4(x) dS(x), \tag{21}$$

where the densities μ_3 and μ_4 are defined as solutions of the inhomogeneous system of linear integral equations:

$$\begin{aligned}
 \mu_3(x) = &\left(a \frac{\partial}{\partial n(x)} + b\right) \left(\frac{2D}{a} \int_{S_3} G_3(x, \xi) \mu_3(\xi) dS(\xi) - 2D \int_{S_4} \frac{\partial G_3(x, \xi)}{\partial n(\xi)} \mu_4(\xi) dS(\xi)\right) \\
 &+ \left(a \frac{\partial}{\partial n(x)} + b\right) T_1(|x|) + c, \tag{22}
 \end{aligned}$$

$$\mu_4(x) = T_1(|x|) + \frac{2D}{a} \int_{S_3} G_3(x, \xi) \mu_3(\xi) dS(\xi) - 2D \int_{S_4} \frac{\partial G_3(x, \xi)}{\partial n(\xi)} \mu_4(\xi) dS(\xi). \tag{23}$$

Proof. For $i \in \{3, 4\}$, each point y_i on the surface S_i may be written, in cylindrical coordinates, as $y_i = ((r_i + \varepsilon_i) \cos \varphi, (r_i + \varepsilon_i) \sin \varphi, z + \varepsilon_{z,i})$, where $\varepsilon_i = \varepsilon_i(\varphi)$ and $\varepsilon_{z,i} = \varepsilon_{z,i}(z)$, with $\varepsilon_{z,i}(z)$ tending to 0 as z tends to $\pm\infty$. This will enable the dependence of the MFPT function on z in $(-\infty, +\infty)$, in addition to those on φ and ρ , which will disappear quickly as z tends to $\pm\infty$. A very important assumption is that Ω_4 , having S_3 and S_4 as boundaries, is contained inside the domain Ω_3 enclosed between S_1 and S_2 . Let σ_3 and σ_4 be the two closed curves obtained as the intersections of the $z = 0$ plane with the surfaces S_3 and S_4 , respectively, so that they turn out to be small deformations of two concentric circles σ_1 and σ_2 , respectively. The common center of such circles σ_1 and σ_2 plays the role of an approximate center of symmetry for σ_3 and σ_4 .

Let $T_1(|y|)$ be the circularly symmetric MFPT function defined in (4) for any y in Ω_1 , with the Dirichlet and Robin boundary conditions on σ_2 and σ_1 , respectively. Let

$G_3(y, y') = \frac{1}{4\pi D|y - y'|}$ be the standard three-dimensional Green's function solution of $D\Delta_y G_3(y, y') = -\delta(y - y')$ in the whole space, without any sort of Dirichlet or Robin boundary conditions. The expansion of G_3 in cylindrical coordinates $w = (\rho, \varphi, z)$ is given by

$$G_3(w, w') = \frac{1}{4\pi D} \sum_{n=-\infty}^{+\infty} e^{in(\varphi-\varphi')} \int_0^{+\infty} e^{-\kappa|z-z'|} J_n(\kappa\rho) J_n(\kappa\rho') d\kappa, \tag{24}$$

where J_n defines the standard regular Bessel functions of the n th order; see [19]. Let $\int_{S_i} dS(x)$ denote integration over the surface S_i for $i \in \{3, 4\}$. By extending the treatment of scenario 2 to the actual three-dimensional situation, it follows that the MFPT function $T_4(y)$ satisfying (3) for y inside Ω_4 , with the Dirichlet and Robin boundary conditions on S_4 and S_3 , respectively, is defined by (21), where the densities μ_3 and μ_4 are defined in S_3 and S_4 , respectively, by the inhomogeneous system of linear integral Equations (22) and (23), respectively. \square

Further information regarding the understanding of the densities μ_3 and μ_4 defined in (22) and (23), respectively, is given in Appendix C.

4. Discussion

The time-honored problem of adequately analyzing elliptic partial differential equations (in particular, in two and three spatial dimensions) inside a domain with a general boundary and prescribed boundary conditions continues to stand as an important and difficult one. The subject by itself has a full variety of important applications, in addition to cell migration. We refer, for instance, to the Kellogg monograph [20] for a detailed investigation of elliptic equations, and we also incorporate previous research by other authors and their applications to electrostatics. Moreover, Balian and Bloch extended those research investigations to the Schrödinger equation in the framework of nuclear physics in [21], and Morse and Feshbach incorporated them for general and useful presentations in [19]. The elliptic partial differential equation is separable only for a few shapes of the boundary; see [19]. Then, for generic geometries of the boundary preventing separability, adequate mathematical methods, giving rise to approximations, have to be developed.

More than one century ago, the analysis of the Laplace equation inside a three-dimensional domain, bounded by one arbitrary surface and either Dirichlet or Neumann boundary conditions (all of which are known as potential theory), was reduced by mathematicians to solve a suitable inhomogeneous linear integral equation of the Fredholm type for certain unknown density functions defined on the surface; see [20]. Such an integral equation provides, at least, a mathematical basis for all cases where the shape of the surface prevents separability (in practice, this includes almost all geometries). In a previous publication [15], the random motion of a tumor cell in a tissue had given rise to the study of a three-dimensional Poisson equation for the MFPT function of the tumor cell inside a domain limited by one or two surfaces. By nontrivially extending [21] to that Poisson equation, the analysis of the three-dimensional MFPT yielded suitable systems of coupled inhomogeneous Fredholm linear integral equations for the corresponding density functions. Cases with spherical surfaces have been solved consistently with solutions found through other methods. Moreover, the approach has been extended to deal with a special variety of nontrivial problems: those for one closed surface with mixed Dirichlet–Neumann boundary conditions on the latter; see [15].

The three-dimensional studies in [15] left open, among a number of other problems, the analysis of two-dimensional cases, in which the boundary is a closed curve, and of three-dimensional cases with cylindrical-like boundaries. These two cases constitute the motivation for and the subject of the present work. In fact, the analysis of the Laplace and Poisson equations in a two-dimensional annulus displays certain peculiarities, which are

not found in three-dimensional annular cylinders and require the specific study carried out here. So, the present work deals with an approach, in the latter geometries, to the MFPT of a migrating cell based upon the two-dimensional extension of the inhomogeneous linear integral equations with the boundaries indicated above. In the present work, we also treat another boundary condition suggested by and relevant for cell migration, namely, the Robin one. The assumed Robin boundary condition describes how cells interact with the inner boundary of the domain, and it combines elements of both fixed values (Dirichlet) and flux (Neumann) conditions so that it accounts for factors like adhesion, chemotaxis, or mechanical forces at the inner boundary, thereby influencing cell behavior and movement. Here, we treat boundaries that are small deformations of others and yield separability: this enables the inhomogeneous linear integral equations to be solved analytically. Theorems 1 and 2 characterize the solutions of the integral equations yielding the MFPT and the corresponding densities, in the deformed two-dimensional boundary and three-dimensional one, respectively.

We quote several problems that are left open in the mathematically oriented approach reported in this work and in [15], such as the following:

- Extensions to more general nonseparable two- and three-dimensional boundaries, which are not small deformations of the separable boundaries considered here;
- Further analysis of mixed boundary conditions on the same boundary.

5. Conclusions

The MFPT function $T(y)$ for a cell, being originated at time $t = 0$ at y in the domain Ω , to reach a suitable part of the boundary of Ω has been studied in different two- and three-dimensional simplified (separable to nonseparable) models considering the Dirichlet and Robin boundary conditions. Drift motion was taken in a general formulation in the two-dimensional case, although it was omitted for simplicity in certain cases. The following models were studied:

- In the two-dimensional case, the domain Ω was defined as an annulus, and the boundary was formed by either two concentric circles or by small deformations thereof;
- In the three-dimensional case, the domain Ω was defined as an annular cylinder, and the boundary was formed by either parallel concentric cylindrical surfaces of finite length or by lengthy deformations thereof.

Explicit solutions have been given for separable cases. By starting from a specific separable model, the corresponding nonseparable one follows, which is generated by slightly deforming the surface of the former. The solution of the Poisson equation for the MFPT function for the slightly deformed boundary has been represented by invoking potential theory in terms of linear integral equations with inhomogeneous terms given by the exact MFPT function of the separable boundary. The use of the exact MFPT functions of the separable boundaries as inhomogeneous terms for the deformed cases constitutes an important achievement. The linear integral equations display similar structures for the chosen deformed geometries and have been solved (reduced to a finite number of quadratures and series summations) for small deformations in outline. The Green's functions involved in those equations for deformed geometries display certain ambiguities, which were analyzed and bypassed using a consistent "averaging" procedure.

Author Contributions: Conceptualization, H.S. and R.F.Á.-E.; methodology, H.S. and R.F.Á.-E.; validation, H.S. and R.F.Á.-E.; formal analysis, H.S. and R.F.Á.-E.; investigation, H.S. and R.F.Á.-E.; resources, H.S. and R.F.Á.-E.; writing original draft and preparation, H.S. and R.F.Á.-E.; writing review and editing, H.S. and R.F.Á.-E.; visualization, H.S. and R.F.Á.-E.; supervision, H.S. and R.F.Á.-E. All authors have read and agreed to the published version of the manuscript.

Funding: This research received no external funding.

Data Availability Statement: No new data were used or created in this manuscript.

Acknowledgments: R.F.Á.-E. acknowledges the Departamento de Física Teórica, Facultad de Ciencias Físicas, Universidad Complutense de Madrid for their hospitality. He is an associate member of the Instituto de Biocomputación y Física de los Sistemas Complejos, Universidad de Zaragoza, Zaragoza, Spain.

Conflicts of Interest: The authors declare no conflict of interest.

Appendix A. The Green’s Function G vs. $G|_{|\nu|=0}$ in Two Dimensions

In this appendix, it is deduced that the Green’s functions G and $G|_{|\nu|=0}$ have the same short-distance behavior due to the fact that the operator $\nu \cdot \nabla$ is a weak perturbation of Δ . Consider the polar coordinates $w = (\rho, \varphi)$, wherein the two-dimensional Green’s function G , the solution of Equation (10), may be expanded into a Fourier series as

$$G(w, w') = \frac{1}{2\pi} \sum_{n=-\infty}^{+\infty} g_n(\rho, \rho') e^{in(\varphi-\varphi')}, \tag{A1}$$

and given the radial Green’s functions $g_n(\rho, \rho')$, for $n \in \mathbb{N}$, we have the solution

$$D \left(\frac{1}{\rho} \frac{\partial}{\partial \rho} \left(\rho \frac{\partial}{\partial \rho} \right) - |\nu| \frac{\partial}{\partial \rho} - \frac{n^2}{\rho^2} \right) g_n(\rho, \rho') = -\frac{1}{\rho} \delta(\rho - \rho'), \tag{A2}$$

which can be obtained directly though general recipes in terms of two linearly independent solutions, $g_{n,re}(\rho)$ regular and $g_{n,ir}(\rho)$ irregular, at $\rho = 0$ of the homogeneous equation

$$D \left(\frac{1}{\rho} \frac{\partial}{\partial \rho} \left(\rho \frac{\partial}{\partial \rho} \right) - |\nu| \frac{\partial}{\partial \rho} - \frac{n^2}{\rho^2} \right) g_{n,j}(\rho) = 0 \tag{A3}$$

with $j \in \{re, ir\}$ (see, for instance, [19] (volume 1)). Therefore,

$$g_n(\rho, \rho') = -D \frac{g_{n,re}(\rho)g_{n,ir}(\rho')\chi(\rho - \rho') + g_{n,ir}(\rho')g_{n,re}(\rho)\chi(\rho' - \rho)}{\rho \Delta(g_{n,re}(\rho), g_{n,ir}(\rho))} \tag{A4}$$

where $\Delta(g_{n,re}(\rho), g_{n,ir}(\rho))$ is the standard (constant) Wronskian of $g_{n,re}(\rho)$ and $g_{n,ir}(\rho)$, and χ is the step function given by $\chi(r) = 0$ for $r < 0$, where $\chi(r) = 1$ if $r > 0$.

When there is no drift, that is, $|\nu| = 0$, the Green’s function G given in (11) is such that

$$\begin{aligned} g_0(\rho, \rho')|_{|\nu|=0} &= -\frac{1}{D} \ln \rho_{max}, & g_{n,re}(\rho) &= \rho^n, \quad n \in \mathbb{Z} \setminus \{0\}, \\ g_n(\rho, \rho')|_{|\nu|=0} &= \frac{1}{2D|n|} \left(\frac{\rho_{min}}{\rho_{max}} \right)^{|n|}, & g_{n,ir}(\rho) &= \rho^{-n}, \quad n \in \mathbb{Z} \setminus \{0\}, \end{aligned} \tag{A5}$$

where $\rho_{min} = \min\{\rho, \rho'\}$, and $\rho_{max} = \max\{\rho, \rho'\}$.

Now, when $|\nu| \neq 0$, if $n = 0$, the two independent solutions of Equation (A3) are $g_{0,re}(\rho) = 1$ and $g_{0,ir}(\rho) = \int_0^\rho \frac{e^{|\nu|\xi}}{\xi} d\xi$; and if $n \neq 0$, then Equation (A3) can be reduced by extending the procedure to yield (6) with a suitable replacement of $-\frac{1}{D}$ to define the linear integral equations. For a recent related application of this technique, see [22]. Namely, let $-\frac{1}{D}$ be replaced by $\frac{n^2}{\rho^2} g_{n,i}(\rho)$ so that the regular (re) solution may be written as

$$g_{n,re}(\rho) = 1 + \int_0^\rho \frac{e^{|\nu|\xi}}{\xi} \left(\int_0^\xi e^{-|\nu|z} n^2 g_{n,re}(z) dz \right) d\xi, \tag{A6}$$

and the irregular (ir) solution may written as

$$g_{n,ir}(\rho) = \int_0^\rho \frac{e^{|\nu|\xi}}{\xi} d\xi + \int_0^\rho \frac{e^{|\nu|\xi}}{\xi} \left(\int_0^\xi e^{-|\nu|z} n^2 g_{n,ir}(z) dz \right) d\xi. \tag{A7}$$

These two integral equations are some sorts of generalizations of Volterra integral equations [23]. Their successive iterations have been analyzed and, some consequences are summarized below. First, the series formed by the successive iterations of Equation (A6) is finite for any ρ , and it tends to 1 as ρ tends to 0. Secondly, the series formed by the successive iterations of Equation (A7), except for the first term, is finite for any ρ , and it tends to 0 as ρ tends to 0, while the first term $\int_0^\rho \frac{e^{|\nu|\xi}}{\xi} d\xi$ tends to $\ln \rho$ as ρ tends to 0. Finally, it follows that G and $G|_{|\nu|=0}$ have the same short-distance behavior.

Appendix B. An Approximation Method for σ_3 and σ_4 Close to σ_1 and σ_2

The system where the densities μ_1 and μ_2 are defined, by Equations (8) and (9), respectively, may be rewritten compactly as

$$\mu = L(T_1) + K(\mu), \tag{A8}$$

where μ is a column vector formed by μ_1 and μ_2 , and

$$L(T_1) = \begin{pmatrix} \left(a \frac{\partial}{\partial n(\xi)} + b \right) T_1 + c \\ T_1 \end{pmatrix},$$

$$K(\mu) = 2D \begin{pmatrix} \left(\frac{\partial}{\partial n(\xi)} + \frac{b}{a} \right) \int_{\sigma_3} G(\xi, s) d\sigma(s) & - \left(a \frac{\partial}{\partial n(\xi)} + b \right) \int_{\sigma_4} \frac{\partial G(\xi, s)}{\partial n(\xi)} d\sigma(s) \\ \frac{1}{a} \int_{\sigma_3} G(\xi, s) d\sigma(s) & - \int_{\sigma_4} \frac{\partial G(\xi, s)}{\partial n(\xi)} d\sigma(s) \end{pmatrix} \begin{pmatrix} \mu_1(s) \\ \mu_2(s) \end{pmatrix}.$$

A posteriori, if $\sigma_i = \sigma_{i-2}$, with $i \in \{3, 4\}$, then $L(T_1)$ evaluated on σ_{i-2} vanishes, and the solutions of the above equations are $\mu_1 = 0$ and $\mu_2 = 0$. Let σ_3 and σ_4 be small deformations of σ_1 and σ_2 , respectively, so that, for each y_i on σ_i , it may be written in polar coordinates $y_i = (r_{i-1} + \varepsilon_i)(\cos \varphi, \sin \varphi)$, with $\varepsilon_i = \varepsilon_i(\varphi)$. Then, $L(T_1)$, now evaluated on σ_3 and σ_4 and no longer on σ_1 and σ_2 , is small, and so μ_1 and μ_2 should be small as well. The integration over σ_3 and σ_4 is carried out as $\int_0^{2\pi} r_1 d\varphi$ and $\int_0^{2\pi} r_2 d\varphi$, respectively. Moreover, the line integrals, the Green’s function G , and its derivative in Equations (8) and (9) can also give rise, to the lowest order, to explicit corrections of the same order (ε_i) as $L(T_1)$. Such corrections can be directly written, but they will be omitted for brevity. Therefore, the previous Equation (A8) may be approximated as

$$\mu \simeq L'(T_1) + K'(\mu), \tag{A9}$$

where $L'(T_1)$ is the sum of $L(T_1)$ and all such corrections, and the operator K' is the resulting approximation of K , which is formed by the line integrals over σ_1 and σ_2 . Corrections to K' are omitted, as they would yield higher corrections to μ . On the other hand, it is not warranted that higher iterates of (A9) have smaller orders of magnitude than lower order ones, that is, all iterates of (A9) should be considered in principle on equal footing. A simpler version of this feature was met for the second term on the right-hand side of Equation (16). Then, the required approximation of (A8), which takes into account all such iterates, is

$$\mu \simeq [I - K']^{-1} L'(T_1), \tag{A10}$$

where I stands for the identity operator, and $[I - K']^{-1}$ denotes the inverse of the operator $I - K'$. For convenience, the components of $L'(T_1)$ are expanded in a Fourier series as

$$L'(T_1)_i = \frac{1}{2\pi} \sum_{n=-\infty}^{+\infty} L'(T_1)_{i,n} e^{in\varphi_i} \tag{A11}$$

with $i \in \{1, 2\}$. The small $L'(T_1)_i$ depend on φ_i , since they are now evaluated on the slightly deformed curves σ_3 and σ_4 . If $n \neq 0$, then $L'(T_1)_{i,n}$ are nonvanishing in general. Suppose that $|v| = 0$ (no drift) so that Equation (A1) applies, and

$$\mu_i(y_i) = \frac{1}{2\pi} \sum_{n=-\infty}^{+\infty} \mu_{i,n} e^{in\varphi_i} \tag{A12}$$

with $i \in \{1, 2\}$. By using Equations (A12) and (A5) and integrating over the angles, it follows from (A9) that the unknown $\mu_{i,n}$, with $\rho_1 = \rho'_1 = r_3$ and $\rho_2 = \rho'_2 = r_4$, are defined by

$$\begin{aligned} \mu_{1,n} &= L'(T_1)_{1,n}(\rho_1) + \frac{2D}{a} r_3 \left(a \frac{\partial g_n(r_3, \rho'_1)}{\partial \rho_1} + b g_n(\rho_1, \rho'_1) \right) \mu_{1,n} + \\ &+ 2D r_4 \left(\left(a \frac{\partial}{\partial \rho_1} \Big|_{\rho_1=r_3} + b \right) \frac{\partial g_n(\rho_1, r_4)}{\partial \rho'_2} \right) \mu_{2,n} \end{aligned} \tag{A13}$$

$$\mu_{2,n} = L'(T_1)_{2,n}(\rho_2) + \frac{2D}{a} r_3 g_n(\rho_2, \rho'_1) \mu_{1,n} + 2D r_4 \frac{\partial g_n(\rho_2, r_4)}{\partial \rho'_2} \mu_{2,n}. \tag{A14}$$

The derivatives $\frac{\partial g_n(r_3, \rho'_1)}{\partial \rho_1}$ and $\frac{\partial g_n(\rho_2, r_4)}{\partial \rho'_2}$ are ambiguous and, thus, pose a problem similar to the one met in Example 1. Then, the ‘‘averaging’’ recipe in such an example has to be invoked as well. The recipe was applied there, in a simpler context, for $n = 0$, and proceeds similarly here for any integer n . For $n = 0$, it follows $\frac{\partial g_0(r_3, \rho'_1)}{\partial \rho_1} = -\frac{1}{2Dr_3}$ and $\frac{\partial g_0(\rho_2, r_4)}{\partial \rho'_2} = -\frac{1}{2Dr_4}$. For $n \neq 0$, it follows $\frac{\partial g_n(r_3, \rho'_1)}{\partial \rho_1} = 0$ and $\frac{\partial g_n(\rho_2, r_4)}{\partial \rho'_2} = 0$. The remaining contributions in the right-hand sides of Equations (A13) and (A14) pose no ambiguity, as $r_4 > r_3$ is directly evaluated. After that, such equations constitute an inhomogeneous algebraic linear system for each pair $\mu_{1,n}$ and $\mu_{2,n}$, which is solved trivially in terms of $L'(T_1)_{1,n}$ and $L'(T_1)_{2,n}$, respectively. Such solving implements the instruction $[I - K']^{-1}$ in Equation (A10). Therefore, the MFPT function reads as

$$T(y) = T'_1(y) + \int_0^{2\pi} r_3 G(y, \xi) \mu_1(\xi) d\varphi + \int_0^{2\pi} r_4 \frac{\partial G(y, \xi)}{\partial n(\xi)} \mu_2(\xi) d\varphi, \tag{A15}$$

where T'_1 includes T_1 and all corrections of the order δ_i that are not included in μ_i .

Appendix C. Extending the Approximation Method to Three Dimensions

To go somewhat deeper into the consistency between the two- and the three-dimensional cases, further information regarding the understanding of Equations (22) and (23) is provided in this appendix. The system formed by Equations (22) and (23) can be recast compactly as

$$\mu = P(T_1) + Q(\mu)$$

where μ is a column vector formed by μ_3 and μ_4 , $P(T_1)$ is a column vector formed by all the contributions related to T_1 , and Q is the 2×2 matrix linear operator containing only surface integrals over S_3 and S_4 . By arguing as in the previous Appendix B, even if the actual counterpart of Equation (A8) is valid for S_3 and S_4 , which are moderate deformations of S_1 and S_2 , respectively, in the following development, it will be assumed that the former two surfaces are small deformations of the latter. Notice that the surface integrals and the functions G_3 and $\frac{\partial G_3}{\partial n}$ in (21)–(23) can also give rise, to the lowest order, to explicit

corrections of the same order (ε_i and $\varepsilon_{z,i}$) as $P(T_1)$. Such corrections can be directly written, as they are independent on μ , but they will be omitted for brevity. The sum of $P(T_1)$ and all such corrections will be denoted by $P'(T_1)$ (of the orders ε_i and $\varepsilon_{z,i}$). Then, for the three-dimensional case, the Equation (A8) can be approximated as

$$\mu \simeq P'(T_1) + Q'\mu, \tag{A16}$$

where Q' is the resulting approximation of Q , and the surface integrals over S_3 and S_4 are approximated by

$$\int_{S_i} = \int_0^{2\pi} \int_{-\infty}^{+\infty} r_i dz_i d\varphi_i,$$

with $i \in \{3, 4\}$. The presence of an integration over \mathbb{R} recalls the three-dimensional nature of the very lengthy, slightly deformed cylinders. With respect to this approximation, the normal derivatives are z -independent and, thus, are similar to those met for Q' in two dimensions. Then, the required approximation of (A16), which takes into account all such iterates, is $\mu \simeq [I - Q']^{-1}P'(T_1)$.

Indeed, by extending the operator in (A11) to the three-dimensional case, the components of $P'(T_1)$ are

$$P'(T_1)_i = \frac{1}{(2\pi)^{3/2}} \int_{-\infty}^{+\infty} \sum_{n=-\infty}^{+\infty} P'(T_1)_{i,n}(k_z) e^{i(n\varphi_1 + zk_z)} dk_z. \tag{A17}$$

The small $P'(T_1)_i$ depend on ρ_i , z and φ_i , with $i \in \{1, 2\}$, since evaluations now are performed on the slightly deformed S_i and, moreover, there are small contributions from the integrals, as discussed previously in the proof of Theorem 2. Let

$$\mu_i(y_i) = \frac{1}{(2\pi)^{3/2}} \int_{-\infty}^{+\infty} \sum_{n=-\infty}^{+\infty} \tilde{\mu}_{i,n}(k_z) e^{i(n\varphi_1 + zk_z)} dk_z \tag{A18}$$

for $i \in \{3, 4\}$. By using Equations (A12) and (A5), and integrating with

$\int_0^{2\pi} \int_{-\infty}^{+\infty} e^{-i(n\varphi_1 + zk_z)} d\varphi_1 dz$, Equation (A16) become ($\rho_1 = \rho'_1 = r_1, \rho_2 = \rho'_2 = r_2$):

$$\begin{aligned} \tilde{\mu}_{3,n}(k_z) = P'(T_1)_{1,n}(k_z) + \frac{2D}{a} r_1 \tilde{\mu}_{3,n}(k_z) & \left(a \int_0^{+\infty} \frac{\kappa}{\kappa^2 + k_z^2} \frac{dJ_n(\kappa\rho)}{d\rho} \Big|_{\rho=r_1} J_n(\kappa r_1) d\kappa + \right. \\ & \left. + b \int_0^{+\infty} \frac{\kappa}{\kappa^2 + k_z^2} J_n(\kappa r_1) J_n(\kappa r_1) d\kappa \right) + \\ & + 2Dr_2 \tilde{\mu}_{4,n}(k_z) \left(a \int_0^{+\infty} \frac{\kappa}{\kappa^2 + k_z^2} \frac{dJ_n(\kappa\rho)}{d\rho} \Big|_{\rho=r_1} \frac{dJ_n(\kappa\rho)}{d\rho} \Big|_{\rho=r_2} d\kappa + \right. \\ & \left. + b \int_0^{+\infty} \frac{\kappa}{\kappa^2 + k_z^2} J_n(\kappa r_1) \frac{dJ_n(\kappa\rho)}{d\rho} \Big|_{\rho=r_2} d\kappa \right) \end{aligned} \tag{A19}$$

$$\begin{aligned} \tilde{\mu}_{4,n}(k_z) = P'(T_1)_{2,n}(k_z) + \frac{2D}{a} r_1 \tilde{\mu}_{3,n}(k_z) & \int_0^{+\infty} \frac{\kappa}{\kappa^2 + k_z^2} J_n(\kappa r_1) J_n(\kappa r_2) d\kappa + \\ & + 2D r_2 \tilde{\mu}_{4,n}(k_z) \int_0^{+\infty} \frac{\kappa}{\kappa^2 + k_z^2} J_n(\kappa r_2) \frac{dJ_n(\kappa\rho)}{d\rho} \Big|_{\rho=r_2} d\kappa. \end{aligned} \tag{A20}$$

The behavior of the previous integrals may be summarized below, with the properties of the Bessel functions involved at small and large κ :

1. The oscillating behavior of the Bessel functions enables the four integrals to be finite at large κ .
2. For small κ and $k_z \neq 0$, all integrals are finite.
3. For small κ and $k_z = 0$, all integrals are finite, except the first one defining $\tilde{\mu}_{4,0}$, which gives rise to a logarithmic divergence. This logarithmic divergence turns out

to be harmless and to yield finite results upon performing integrations over k_z at a later stage.

4. The first integral defining $\tilde{\mu}_{3,n}$ and the last one defining $\tilde{\mu}_{4,n}$ pose ambiguities related to those met in Example 1 and in the proof of Theorem 2. In fact, by invoking the asymptotic behavior of the Bessel functions for large κ , the oscillating integrands in those two integrals are shown to contain contributions having, to the leading order, the same asymptotic behavior in κ as the oscillating integrand of the integral $U(\rho - \rho') = \int_{\kappa_0}^{+\infty} \frac{\sin(\rho - \rho')\kappa}{\kappa} d\kappa$, with large but finite κ_0 . $U(\rho - \rho')$ is finite and nonvanishing for $\rho - \rho' \neq 0$, it changes sign as $\rho - \rho'$ does, and $U(0) = 0$.

An alternative argument supporting the discontinuity and, hence, the ambiguity, is the following: for $\rho - \rho' > 0$, one has $U(\rho - \rho') = -\text{si}(\kappa_0(\rho - \rho'))$, with $\text{si}(z)$ being a function related to the sine-integral function (Equation (5.2.26) in [24]). Notice that $\text{si}(z)$ is unambiguously defined if $|\text{argument}(z)| < \pi$, but $z = \kappa_0(\rho - \rho') < 0$ (say, $\text{argument}(z) = \pi$) precisely for $\rho - \rho' < 0$.

Then, those two integrals contain contributions having different (finite and nonvanishing) values depending on the sign of $\rho - \rho'$. They have to be evaluated by the same “averaging” procedure. For instance, the integral $\int_0^{+\infty} \frac{\kappa J_n(\kappa r_2)}{\kappa^2 + k_z^2} \frac{dJ_n(\kappa r_2)}{d\rho'} d\kappa$ has to be replaced by

$$\frac{1}{2} \left(\int_0^{+\infty} \frac{\kappa J_n(\kappa(r_2 + \epsilon))}{\kappa^2 + k_z^2} \frac{dJ_n(\kappa r_2)}{d\rho'} d\kappa + \int_0^{+\infty} \frac{\kappa J_n(\kappa(r_2 - \epsilon))}{\kappa^2 + k_z^2} \frac{dJ_n(\kappa r_2)}{d\rho'} d\kappa \right),$$

with $\epsilon > 0$ tending to 0, a procedure which cancels out the different contributions with opposite signs. And so on for the other integral.

5. The third integral in $\tilde{\mu}_{3,n}$ and the first one in $\tilde{\mu}_{4,n}$ above behave in a continuous way and do not give rise to ambiguities.

After that, Equations (A19) and (A20) constitute an inhomogeneous algebraic linear system for each pair $\tilde{\mu}_{3,n}$ and $\tilde{\mu}_{4,n}$, which is solved trivially in terms of $P'(T_1)_{1,n}$ and $P'(T_1)_{2,n}$, respectively. That implements the instruction $\mu \simeq [I - Q']^{-1}P'(T_1)$ at the end of the proof of Theorem 2. The resulting $\tilde{\mu}_{3,n}$ and $\tilde{\mu}_{4,n}$ yield, through Equations (A15), (A18), and (24), the MFPT function.

The limiting case $S_i = S_{i-2}$, with $i \in \{3, 4\}$, (z dependence thereby disappearing) will be revisited briefly, to provide further consistency between the two- and three-dimensional cases without deformations. Notice the following relationship between the three- and two-dimensional Green’s functions without boundary surfaces $\int_{-\infty}^{+\infty} G_3(y, y') dz' = G(y, y')$, where y and y' in the left-hand and right-hand sides are three-dimensional and two-dimensional, respectively. Then, by invoking Equations (24) and (A1), it follows the interesting relationship involving Bessel functions:

$$\frac{1}{D} \int_0^{+\infty} \frac{1}{\kappa} J_n(\kappa\rho) J_n(\kappa\rho') d\kappa = g_n(\rho, \rho'). \tag{A21}$$

This enables us to follow the correspondence between Equations (8) and (9), between (22) and (23), between Equations (A13) and (A14), and between (A19) and (A20) to hence to confirm consistency. The details are omitted.

Similarly, the MFPT function solution of (17) becomes

$$T_3(y) = T'_1(y) + \frac{2D}{a} \int_{S_1} G_3(y, \xi) \mu_3(\xi) dS(\xi) - 2D \int_{S_2} \frac{\partial G_3(y, \xi)}{\partial n(\xi)} \mu_4(\xi) dS(\xi), \tag{A22}$$

where T'_1 includes T_1 and the remaining small corrections, which are counterparts of those included into $P'(T_1)$.

References

1. Chambers, A.F.; Groom, A.C.; MacDonald, I.C. Dissemination and growth of cancer cells in metastatic sites. *Nat. Rev. Cancer* **2002**, *2*, 563. [[CrossRef](#)] [[PubMed](#)]
2. Pantel, K.; Brakenhoff, R.H. Dissecting the metastatic cascade. *Nat. Rev. Cancer* **2004**, *4*, 448. [[CrossRef](#)] [[PubMed](#)]
3. Chaffer, C.L.; Weinberg, R.A. A perspective on cancer cell metastasis. *Science* **2011**, *331*, 1559. [[CrossRef](#)] [[PubMed](#)]
4. Hanahan, D.; Weinberg, R.A. The hallmarks of cancer: The next generation. *Cell* **2011**, *144*, 646. [[CrossRef](#)] [[PubMed](#)]
5. Fedotov, S.; Iomin, A. Migration and Proliferation Dichotomy in Tumor-Cell Invasion. *Phys. Rev. Lett.* **2007**, *98*, 118101. [[CrossRef](#)] [[PubMed](#)]
6. Liang, L.; Norrelykke, S.F.; Cox, E.C. Persistent cell motion in the absence of external signals: A search strategy for eukaryotic cells. *PLoS ONE* **2008**, *3*, 1.
7. Dahlenburg, M.; Pagnini, G. Exact calculation of the mean first passage time of continuous-time random walks by nonhomogeneous Wiener-Hopf integral equations. *J. Phys. A Math. Theor.* **2022**, *55*, 505003. [[CrossRef](#)]
8. Redner, S. *A Guide to First-Passage Processes*; Cambridge University Press: Cambridge, UK, 2007.
9. Metzler, R.; Oshanin, G.; Redner, S. *First-Passage Phenomena and Their Applications*; World Scientific: Singapore, 2014.
10. Jacobs, K. *Stochastic Processes for Physicists*; Cambridge University Press: Cambridge, UK, 2010.
11. Condamin, S.; Bénichou, O.; Tejedor, V.; Voituriez, R.; Klafter, J. First-passage times in complex scale-invariant media. *Nature* **2007**, *450*, 77. [[CrossRef](#)]
12. Grebenkov, D.S.; Skvortsov, A.T. Mean first-passage time to a small absorbing target in an elongated planar domain. *New J. Phys.* **2020**, *22*, 113024. [[CrossRef](#)]
13. Grebenkov, D.S.; Rupprecht, J.-F. The escape problem for mortal walkers. *J. Chem. Phys.* **2017**, *146*, 084106. [[CrossRef](#)] [[PubMed](#)]
14. Mangeat, M.; Rieger, H. The narrow escape problem in a circular domain with radial piecewise constant diffusivity. *J. Phys. A Math. Theor.* **2019**, *52*, 424002. [[CrossRef](#)]
15. Serrano, H.; Álvarez-Estrada, R.F.; Calvo, G.F. Mean first-passage time of cell migration in confined domains. *Math. Meth. Appl. Sci.* **2023**, *46*, 7435–7453. [[CrossRef](#)]
16. Risken, H. *The Fokker-Planck Equation*; Springer: Berlin/Heidelberg, Germany, 1996.
17. Hanggi, P.; Talkner, P.; Borkovec, M. Reaction-rate theory: Fifty years after Kramers. *Rev. Mod. Phys.* **1990**, *62*, 251. [[CrossRef](#)]
18. Durand, E. *Electrostatique et Magnetostatique*; Masson: Paris, France 1953.
19. Morse, P.M.; Feshbach, H. *Methods of Theoretical Physics. Part I and Part II*; McGrawHill: New York, NY, USA, 1953.
20. Kellogg, O.D. *Foundations of Potential Theory*; Springer: Berlin/Heidelberg, Germany; New York, NY, USA, 1967; Chapter 11.
21. Balian, R.; Bloch, C. Distribution of Eigenfrequencies for the Wave Equation in a Finite Domain I. Three-Dimensional Problem with Smooth Boundary Surface. *Ann. Phys.* **1970**, *60*, 401–447. [[CrossRef](#)]
22. Singh, R.; Wazwaz, A.-M. An Efficient Method for Solving the Generalized Thomas-Fermi and Lane-Emden-Fowler Type Equations with Nonlocal Integral Type Boundary Conditions. *Int. J. Appl. Comput. Math.* **2022**, *8*, 68. [[CrossRef](#)]
23. Lovitt, W.V. *Linear Integral Equations*; Dover Publications Inc.: Mineola, NY, USA, 1950.
24. Abramowitz, M.; Stegun, I.A. *Handbook of Mathematical Functions with Formulas, Graphs and Mathematical Tables*; National Bureau of Standards Applied Mathematics Series: Washington, DC, USA, 1964; Volume 55.

Disclaimer/Publisher’s Note: The statements, opinions and data contained in all publications are solely those of the individual author(s) and contributor(s) and not of MDPI and/or the editor(s). MDPI and/or the editor(s) disclaim responsibility for any injury to people or property resulting from any ideas, methods, instructions or products referred to in the content.